A Bimetallic Palladium Catalyst for Asymmetric Allylic Substitution Reactions†

Urs Burckhardt,‡ Markus Baumann,‡ Gerald Trabesinger,‡ Volker Gramlich,§ and Antonio Togni*,‡,||

Laboratory of Inorganic Chemistry and Institute of Crystallography and Petrography, Swiss Federal Institute of Technology, ETH-Zentrum, CH-8092 Zürich, Switzerland

Received June 24, 1997⊗

With 1,1′-diacetylruthenocene (**9**) as starting material, the preparation of 1,1′-bis[1-(1-{(*R*)-1-[(*S*)-2-(diphenylphosphino)ferrocenyl]ethyl})-1*H*-pyrazol-3-yl]ruthenocene ((*R*,*R*)-(*S*,*S*)-**12**) is attained in three steps. **12** coordinates to two independent Pd(II)−π-allyl units to form the dicationic complex **15**, isolated as a bis(hexafluorophosphate) salt. This has been characterized by X-ray and 2D NMR methods in solution, along with the analogous derivative **14**, which contains 1-{(*R*)-1-[(*S*)-2-(diphenylphosphino)ferrocenyl]ethyl}-3-ruthenocenyl-1*H*-pyrazole ((*R*)-(*S*)-**8b**). The three Pd(II)−allyl fragments in these two complexes show very similar conformational features. In the Pd-catalyzed substitution reaction of ethyl (1,3-diphenylallyl)carbonate (**1**) with benzylamine, the bimetallic catalyst containing ligand **12** and the mononuclear catalyst formed by **8b** afford the same high enantioselectivity (99.3%).

Introduction

We previously reported the successful application of ferrocenyl ligands of type **3**, containing a phosphine and a pyrazole fragment as coordinating units, in Pd-catalyzed reactions of allylic substrates.[1] In particular, the extremely high enantioselectivity obtained in the substitution reaction of ethyl (1,3-diphenylallyl)carbonate with benzylamine (up to >99.5% ee; see Scheme 1) was ascribed to a synergistic interplay of steric and electronic properties of the ligand and the optimum influence of anionic, cocatalytic species added to the reaction mixture. Thus, the different trans influences exerted by phosphorus and nitrogen on the allylic ligand in the intermediate Pd(II) complex creates a bias toward nucleophilic attack at the carbon atom trans to phosphorus. Such a bias is reinforced by a sterically induced distortion of the allyl fragment (allyl "rotation"), leading to an increased electrophilicity of the same allylic carbon, by virtue of its pronounced out-of-plane position in the intermediate, as shown by first-principle calculations,[2] 2D NMR studies in solution, and X-ray crystal structure analyses.[3] Furthermore, the addition of small potentially coordinating anions, such as fluoride or borohydride, was shown to enhance the selectivity of the system, probably by virtue of a faster equilibration of the diastereoisomeric π-allyl intermediates.[4]

We now extend the study of our ligand system toward the incorporation of more than one catalyst unit into the same molecule. Thereby we are pursuing the goal of well-defined multicenter catalysts that might possibly simplify catalyst recovery and reuse, by virtue of their lower solubility. However, the very high local concentration of single catalyst units might also be detrimental to catalytic activity and selectivity, because of potential intramolecular interaction between the single components leading to a plethora of possible consequences. Among others, the most obvious are deleterious steric interactions and the formation of catalytically inactive di- and polynuclear complexes and aggregates. However, the fortuitous possibility of synergistic effects, though remote, should not be disregarded. With these considerations in mind, and as a first step toward the realization of dendritic[5] asymmetric catalysts, we report here the synthesis and characterization of a Pd bimetallic system[6] as a catalyst for the model allylic substitution reaction of ethyl (1,3-diphenylallyl)carbonate (**1**) with benzylamine.

Scheme 1

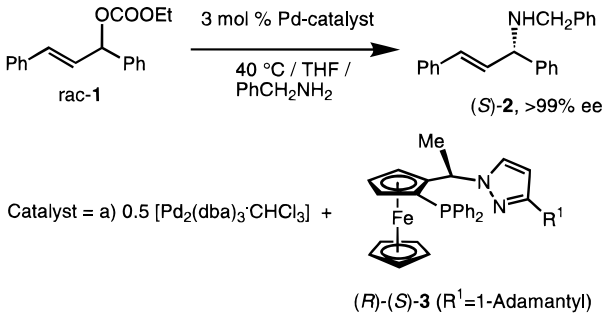

Results and Discussion

Synthesis of Ligands and Complexes. For the best chiral inductions in Pd-catalyzed substitution reactions of 1,3-diphenylallyl derivatives, the P,N chiral ligand must contain a large and compact substituent at the position adjacent to the coordinating nitrogen, 1-adamantyl being exemplary.[1] We found that a fer-

† This paper is dedicated to Professor Dieter Seebach, teacher and colleague, on the occasion of his 60th birthday.

‡ Laboratory of Inorganic Chemistry.
§ Institute of Crystallography and Petrography.
|| E-mail: togni@inorg.chem.ethz.ch.

⊗ Abstract published in *Advance ACS Abstracts,* November 1, 1997.

(1) Togni, A.; Burckhardt, U.; Gramlich, V.; Pregosin, P. S.; Salzmann, R. *J. Am. Chem. Soc.* **1996**, *118*, 1031.
(2) Blöchl, P. E.; Togni, A. *Organometallics* **1996**, *15*, 4125.
(3) Burckhardt, U.; Gramlich, V.; Hofmann, P.; Nesper, R.; Pregosin, P. S.; Salzmann, R.; Togni, A. *Organometallics* **1996**, *15*, 3496.
(4) Burckhardt, U.; Baumann, M.; Togni, A. *Tetrahedron: Asymmetry* **1996**, *8*, 155.

S0276-7333(97)00532-3 CCC: $14.00

Scheme 2[a]

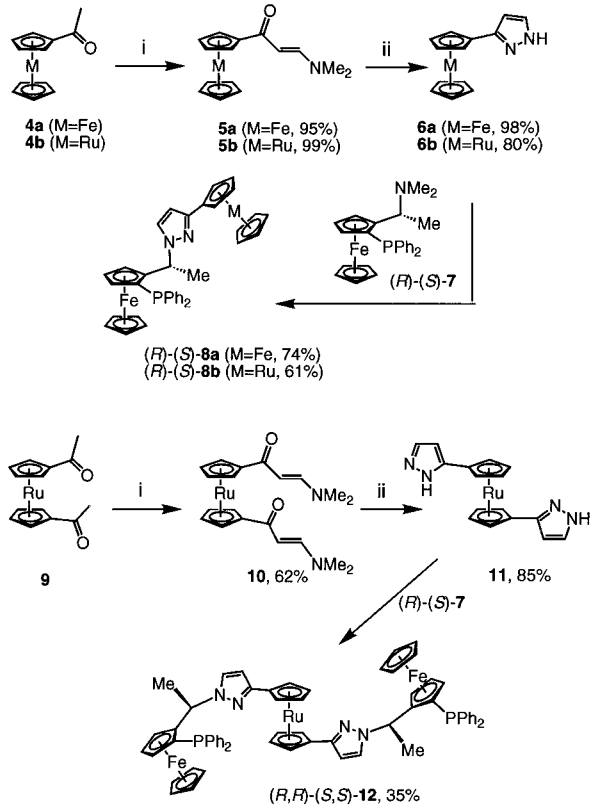

[a] Legend: (i) neat $CH(OMe)_2NMe_2$; (ii) H_2NNH_2/EtOH.

rocenyl or ruthenocenyl group at the same position is almost as beneficial (vide infra). The choice of an extra metallocenyl group was guided by the idea that the latter might be "shared" by two (or, eventually, more) ligand units converging at the central metallocene.[7] This fragment offers the opportunity of controlling the orientation and relative position of the ligand units, by virtue of its substitution pattern and conformation. Thus, in order to test this idea, mono- and bis(3-1*H*-pyrazolyl)-substituted metallocenes were needed (compounds **6** and **11**, respectively). Their preparation is shown in Scheme 2. In a subsequent step derivatives **6** and **11** were reacted with ferrocenylphosphine **7** in acetic acid,[8] affording the new ligands **8** and **12** in moderate to good yields. No triferrocenyl derivative

Chart 1

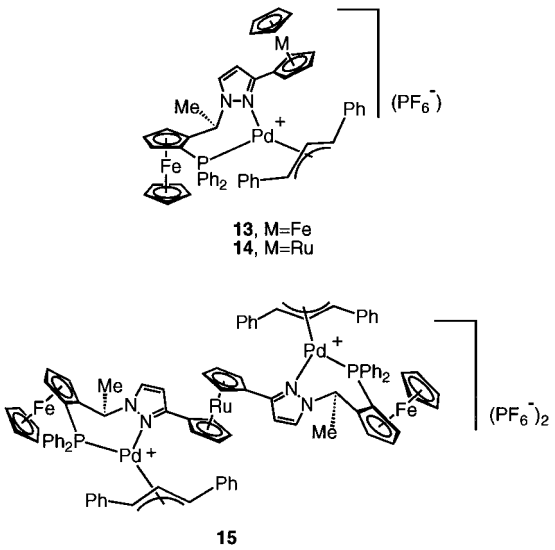

corresponding to **12** was prepared because of the significantly higher selectivity obtained by utilizing **8b** (vs **8a**) in catalytic experiments (vide infra).

Cationic Pd−π-allyl complexes of the type shown in Chart 1 containing the new ligands **8a**, **8b**, and **12**, respectively, were prepared by conventional protocols[1] starting from the chloride-bridged dinuclear derivative $[Pd_2Cl_2(\eta^3\text{-PhCHCHCHPh})_2]$[9] and were isolated in almost quantitative yield as their stable hexafluorophosphate salts.

Solid-State and Solution Structures of 14 and 15. Since cationic Pd(II)−π-allyl complexes are recognized to be key intermediates in Pd-catalyzed substitution reactions and, as previously shown, configurational aspects of such complexes are eminently important in determining stereoselectivity, the solid-state and solution structures of derivatives **14** and **15** have been examined. ORTEP views of the corresponding cations are shown in Figures 1 and 2. Table 1 collects crystal and data collection parameters. A selection of important bond distances, angles, and torsion angles for both compounds are given in Table 2.

The bonding parameters turn out to be rather routine and fall in the expected ranges.[10] Complex cation **15** displays an only approximate C_2 symmetry, with the halves of the molecule being crystallographically inequivalent. For both complexes several structural characteristics that turn out to be quite specific for this class of derivatives are worth noting. Indeed, as previously reported for, for example, the corresponding complex containing ligand **3**,[1] one observes the following key features. The configuration of the π-allyl ligand may be described as *exo-syn-syn*, with the central allylic C−H vector pointing away from the ferrocene core. The three allyl fragments are "rotated" in such a manner that the allylic carbon atoms trans to phosphorus are located at an average distance of 0.507 Å from the

(5) For general reviews on dendrimers, see: (a) Tomalia, D. A.; Naylor, A. M.; Goddard, W. A. G. *Angew. Chem., Int. Ed. Engl.* **1990**, *29*, 138. (b) Tomalia, D. A. *Aldrichim. Acta* **1993**, *26*, 91. (c) Tomalia, D. A.; Durst, H. D. *Top. Curr. Chem.* **1993**, *165*, 193. (d) Issberger, J.; Moors, R.; Vögtle, F. *Angew. Chem.* **1994**, *106*, 2507. (e) Mekelburger, H.-B.; Jaorek, W.; Vögtle, F. *Angew. Chem., Int. Ed. Engl.* **1992**, *31*, 1571. For recent reports concerning metal-containing dendrimers, see: (f) Seebach, D.; Marti, R. E.; Hintermann, T. *Helv. Chim. Acta* **1996**, *79*, 1710. (g) Achar, S.; Puddephatt, R. J. *Angew. Chem., Int. Ed. Engl.* **1994**, *33*, 847. (h) Bhyrappa, P.; Young, J. K.; Moore, J. S.; Suslick, K. S. *J. Am. Chem. Soc.* **1996**, *118*, 5708. (i) Huck, W. T. S.; van Veggel, F. C. J. M.; Reinhoudt, D. N. *Angew. Chem.* **1996**, *108*, 1304. (j) Moulines, F.; Djakovitch, L.; Boese, R.; Gloaguen, B.; Thiel, W.; Fillaut, J.-L.; Delville, M.-H.; Astruc, D. *Angew. Chem., Int. Ed. Engl.* **1993**, *32*, 1075. For the first report on a dendritic homogeneous catalyst, see: (k) Knapen, J. W. J.; van der Made, A. W.; de Wilde, J. C.; Leeuwen, P. W. N. M.; Wijkens, P.; Grove, D. M.; van Koten, G. *Nature* **1994**, *372*, 659.

(6) For recent reports on bimetallic catalysts, see, e.g.: (a) Sawamura, M.; Sudoh, M.; Ito, Y. *J. Am. Chem. Soc.* **1996**, *118*, 3309. (b) Arai, T.; Yamada, Y. M. A.; Yamamoto, N.; Sasai, H.; Shibasaki, M. *Chem. Eur. J.* **1996**, *1996*, 1368. (c) Shibasaki, M.; Sasai, H.; Arai, T. *Angew. Chem., Int. Ed. Engl.* **1997**, *36*, 1237.

(7) For a recent example of a dimeric porphyrin linked by a ferrocenyl unit, see: Burrell, A. K.; Campbell, W.; Officer, D. L. *Tetrahedron Lett.* **1997**, *38*, 1249.

(8) Burckhardt, U.; Hintermann, L.; Schnyder, A.; Togni, A. *Organometallics* **1995**, *14*, 5415.

(9) Hayashi, T.; Yamamoto, A.; Ito, Y.; Nishioka, E.; Miura, H.; Yanagi, K. *J. Am. Chem. Soc.* **1989**, *111*, 6301.

(10) (a) Allen, F. H.; Kennard, O.; Watson, D. G.; Brammer, L.; Orpen, A. G.; Taylor, R. *J. Chem. Soc., Perkin Trans 2* **1987**, Supplement S1−S19. (b) Orpen, A. G.; Brammer, L.; Allen, F. H.; Kennard, O.; Watson, D. G.; Taylor, R. *J. Chem. Soc., Dalton Trans.* **1989**, Supplement S1−S83.

Table 1. Experimental Data for the X-ray Diffraction Study of (*R*)-(*S*)-14 and (*R,R*)-(*S,S*)-15

	(*R*)-(*S*)-**14**	(*R,R*)-(*S,S*)-**15**
formula	$C_{52}H_{46}F_6FeN_2P_2PdRu$	$C_{94}H_{82}F_{12}Fe_2N_4P_4Pd_2Ru\cdot 4CH_2Cl_2\cdot H_2O$
mol wt	1138.2	2402.8
cryst dimens, mm	0.4 × 0.4 × 0.4	0.15 × 0.15 × 0.30
data collecn *T* (°C)	20	20
cryst syst	orthorhombic	monoclinic
space group	$P2_12_12_1$	$P2_1$
a (Å)	14.839(12)	13.336(10)
b (Å)	17.58(2)	27.58(3)
c (Å)	18.11(2)	15.092(13)
β (deg)		99.03(6)
V (Å^3)	4726(8)	5481(8)
Z	4	2
ρ(calcd) (g cm^{-3})	1.600	1.456
μ (cm^{-1})	11.24	10.33
F(000)	2288	2416
diffractometer	Picker-STOE	Syntex P21
radiation	Mo Kα, λ = 0.710 73 Å	Mo Kα, λ = 0.710 73 Å
measured reflns	$0 \le h \le 14$, $0 \le k \le 16$, $0 \le l \le 17$	$0 \le h \le 11$, $0 \le k \le 23$, $-12 \le l \le 12$
2θ range (deg)	3.0−40.0	3.0−35
scan type	ω	ω
scan width (deg)	1.00	1.00
bkgd time (s)	0.15 × scan time	0.10 × scan time
max scan speed (deg min^{-1})	1.0−4.0 in ω	1.5−6.0 in ω
no. of indepnt data coll	2509	3578
no. of obsd rflns (n_o)	2264	2712
	$\|F_o^2\| > 4.0\sigma(\|F\|^2)$	$\|F_o^2\| > 4.0\sigma(\|F\|^2)$
abs corr	face-indexed numerical	N/A
no. of params refined (n_v)	632	485
quantity minimized	$\sum w(F_o - F_c)^2$	$\sum w(F_o - F_c)^2$
weighting scheme	$w^{-1} = \sigma^2(F) + 0.0103\,F^2$	$w^{-1} = \sigma^2(F) + 0.0826\,F^2$
R^a	0.0390	0.0648
$R_w{}^b$	0.0448	0.0899
GOF^c	0.50	0.33

[a] $R = \sum(||F_o| - (1/k)|F_c||)/\sum|F_o|$. [b] $R_w = \sum w(||F_o| - (1/k)|F_c||)^2/[\sum w|F_o|^2]^{1/2}$. [c] GOF $= [\sum w(|F_o| - (1/k)|F_c|)^2/(n_o - n_v)]^{1/2}$. [d] Reflections beyond 2θ = 35° could not be measured due to crystal decomposition (loss of solvent).

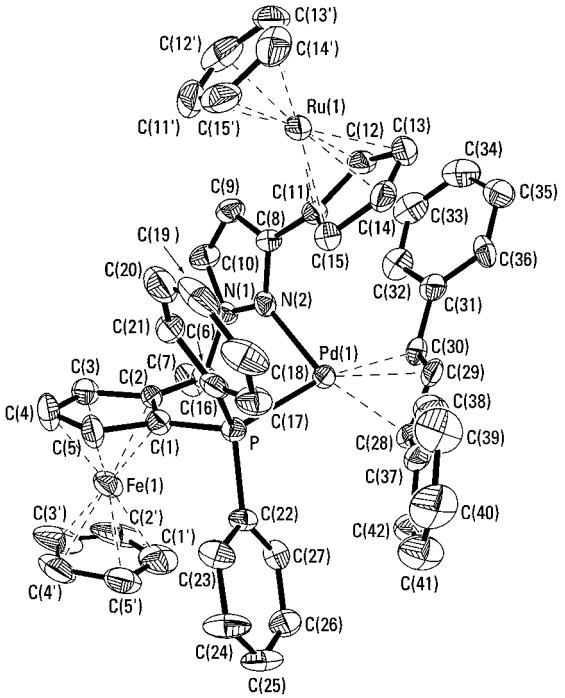

Figure 1. ORTEP view and atom-numbering scheme of the cation of (*R*)-(*S*)-**14**.

respective Pd−N−P plane, whereas their counterparts trans to nitrogen take an almost in-plane position (average distance of 0.08 Å). This distortion is more pronounced for the two allyl ligands in **15** than is the case for **14**.

Figure 3 shows a superposition of the three Pd complex units of **14** and **15**, demonstrating the similarities of their conformational features. The incorporation of a ruthenocenyl(diyl) moiety, as expected, does not influence the relative position of the remaining groups in the molecules, in particular the pseudo-axial orientation of the pyrazole fragment with respect to the substituted ferrocenyl Cp ring. In compound **15** the two pyrazolyl units occupy nearly eclipsed 1,1′ positions on the ruthenocene and the respective planes form angles of 21.3 and 22.9°, respectively, with the planes of the ruthenocenyl Cp rings. The pyrazole planes subtend an angle of only 3.4°, but the orientation of the heterocycles can be viewed as antiparallel. In other words, the central bis(pyrazolyl)ruthenocene unit assumes a chiral C_2-symmetric conformation. This leads to a distal relative position of the two allyl fragments, such that a hypothetical external approach to them will occur in an antiparallel fashion (see Figure 2).

An important question was whether or not the solution structure of the two compounds would correlate with that observed in the solid state. Detailed NMR studies in CD_2Cl_2 solution (^{1}H, ^{13}C, ^{31}P, NOESY, and correlation spectroscopy), as reported previously for similar complexes,[1,3] reveal very similar spectra for **14** and **15**. For both compounds the presence of several species, existing in comparable relative amounts, is observed. Structure assignment was possible for three major isomers, accounting for more than 95% of all species present. On the basis of signal integration, the relative distributions of the three isomeric components **a**−**c** are very similar and account to 100/6/13 for **14** and 100/5/12 for **15**. A selection of important NMR data for these species is given in Table 3, and a complete set of NMR characteristics for **14** and **15** may be found in the

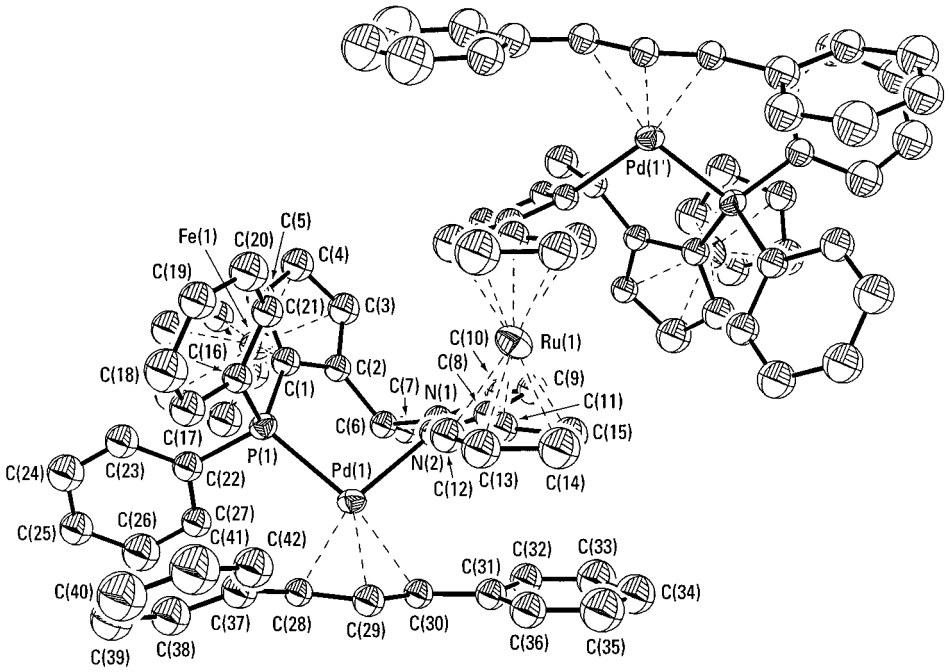

Figure 2. ORTEP view and atom-numbering scheme of the dication of (*R*,*R*)-(*S*,*S*)-**15**.

Table 2. Selected Bond Distances (Å)[a] and Angles (deg)[a] for (*R*)-(*S*)-14 and (*R*,*R*)-(*S*,*S*)-15

	(*R*)-(*S*)-**14**	(*R*,*R*)-(*S*,*S*)-**15**[b]
	Bond Distances	
Pd−P(1)	2.314(3)	2.297(9) [2.300(9)]
Pd−N(2)	2.104(8)	2.092(20) [2.159(22)]
Pd−C(28)	2.161(11)	2.143(25) [2.123(30)]
Pd−C(29)	2.188(10)	2.150(28) [2.133(34)]
Pd−C(30)	2.279(10)	2.340(30) [2.225(32)]
C(28)−C(29)	1.431(15)	1.323(40) [1.364(43)]
C(29)−C(30)	1.395(15)	1.412(43) [1.463(47)]
N(1)−N(2)	1.349(11)	1.375(31) [1.383(33)]
	Bond Angles	
P−Pd−N(2)	92.5(2)	96.6(6) [96.9(7)]
N(2)−Pd−C(30)	97.8(3)	96.4(9) [93.4(10)]
P−Pd−C(28)	102.9(3)	103.0(8) [102.3(8)]
C(28)−C(29)−C(30)	122.2(9)	124.0(28) [120.6(28)]
	Torsion Angles[c]	
C(1)−C(2)−C(6)−N(1)	81	87 [83]
C(2)−C(1)−P−C(16)	126	144 [143]
C(5)−C(1)−P−C(22)	70	88 [84]
C(3)−C(2)−C(6)−C(7)	30	41 [34]
C(2)−C(6)−N(1)−N(2)	79	70 [69]
C(7)−C(6)−N(1)−N(2)	26	17 [18]
C(1)−P−C(16)−C(17)	34	34 [23]

[a] Numbers in parentheses are esd's in the least significant digits. [b] Numbers in brackets are bonding parameters of the second unit. [c] Absolute values.

Supporting Information. The major component **a** displays in both cases the same *exo-syn-syn* configuration of the allyl fragment as observed in the crystal structure. The second diastereoisomer, **b**, shows an *endo-anti-syn* configuration, with the *anti* terminus of the allyl being located trans to nitrogen. Finally, the third identified structure is in an *endo-syn-syn* configuration. However, it is important to note that, as one would expect, the two units of **15** are not distinguishable due to the C_2 symmetry of the molecule. A direct consequence of this is that diastereoisomers of **15** containing the two allyl ligands in different configurations cannot be identified as discrete species. Furthermore, one can conclude that the two Pd−allyl units are fully independent from one another, as if they were unconnected. This

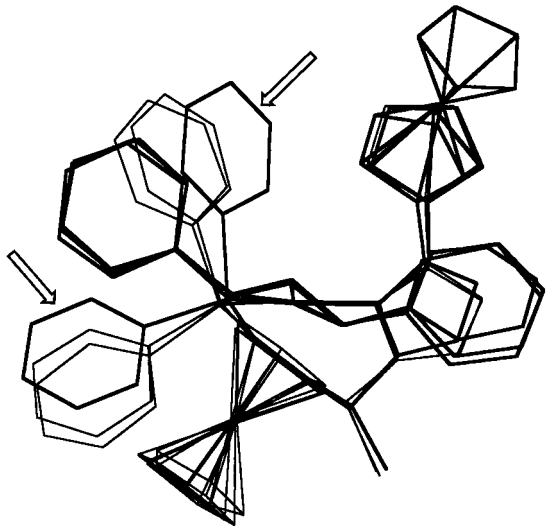

Figure 3. Schematic superposition of **14** with the two units of **15**, showing the great similarity of their conformational features. The arrows indicate the PPh_2 phenyls of **14**.

is also indicated by the cyclic voltammetric characterization (see Supporting Information, Table S1).

The protons attached to position 4 of the pyrazoles in the main isomer appear for **15** at a chemical shift of 5.11 ppm, a significant shielding with respect to their companions in **14** (δ 5.88 ppm). Furthermore, they display a strong NOE to one of the *ortho* phenyl protons of a PPh_2 group. Since this NOE is not observable for **14**, we conclude that this close contact concerns protons not belonging to the same unit. Indeed, from the crystal structure, and as illustrated in Figure 4, the calculated distances between the indicated hydrogen atoms are 2.45 and 2.68 Å, sufficiently short to give rise to strong NOE signals. Thus, one can conclude that the conformation of **15a** in solution is very similar to that observed in the solid state.

Another difference between the di- and trimetallocene derivatives concerns the exchanges observed on the

Table 3. Selected 500 MHz ^{1}H, 125.8 MHz ^{13}C, and 202.6 MHz ^{31}P NMR Data (CD_2Cl_2, Room Temperature) for the Three Major Configurational Isomers of (*R*)-(*S*)-14 and (*R*,*R*)-(*S*,*S*)-15

	exo-syn-syn-**14a**	*endo-anti-syn*-**14b**	*endo-syn-syn*-**14c**	*exo-syn-syn*-**15a**	*endo-anti-syn*-**15b**	*endo-syn-syn*-**15c**
rel distribn	100	6	13	100	5	12
	13.3[a]	12.7[a]	12.2[a]	12.5[a]	11.6[a]	12.6[a]
CH(1)[b]	6.60 (107.2)	5.80 (94.3)	4.60 (90.8)	6.52 (107.2)	5.63 (94.8)	4.48 (91.5)
CH(2)[b]	6.08 (111.5)	5.56 (110.1)	6.84 (109.2)	6.03 (111.2)	6.44 (107.7)	6.80 (109.4)
CH(3)[b]	4.92 (66.3)	6.45 (76.5)	5.11 (81.5)	4.88 (66.6)	6.38 (76.5)	5.08 (81.4)
CH(4)[b]	6.47 (57.4)	5.89 (57.6)	6.01 (57.5)	6.45 (57.6)	5.90 (57.8)	6.06 (57.7)
CH(5)[b]	2.25 (18.2)	1.76 (17.4)	1.90 (17.9)	2.26 (18.2)	1.80 (17.5)	1.93 (17.6)
CH(6)[b]	4.07 (74.2)	4.07	3.99	4.13 (74.3)	4.05 (73.3)	4.12
CH(7)[b]	4.48 (71.3)	4.51	4.47	4.54 (71.3)	4.52 (71.4)	4.51 (71.4)
CH(8)[b]	4.66 (66.9)	4.66	4.68	4.76 (67.4)	4.73 (67.5)	4.69 (68.9)
CH(9)[b]	7.52 (128.3)	7.22	7.25	7.38 (129.0)	7.49	7.13
CH(10)[b]	5.88 (108.8)	5.86 (108.3)	5.89 (108.8)	5.11 (107.9)	5.42 (108.6)	5.23 (107.7)
η^5-C_5H_5 (Fc)	3.84 (71.3)	3.98	3.76 (73.2)	3.83 (71.4)	3.97	3.75
η^5-C_5H_5 (Rc)	4.24 (71.8)	4.32	4.38 (70.8)			

[a] $\delta(^{31}P)$. [b] $\delta(^1H)$ ($\delta(^{13}C)$). The arbitrary numbering scheme is as follows:

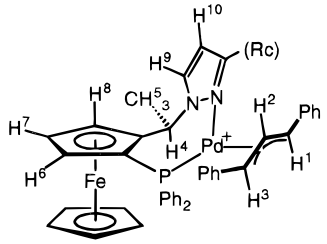

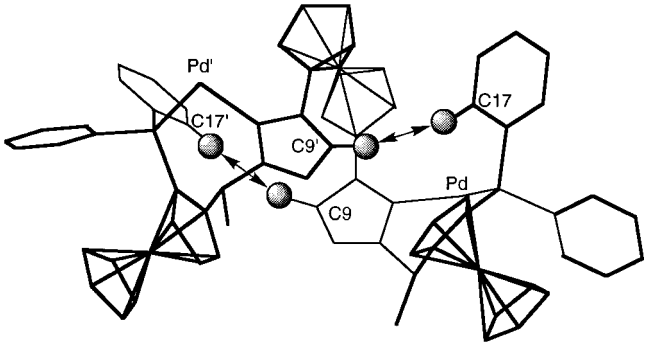

Figure 4. Schematic representation of the crystal structure of **15**, showing the two pairs of hydrogen atoms in their calculated positions, for which a strong NOE has been observed in solution.

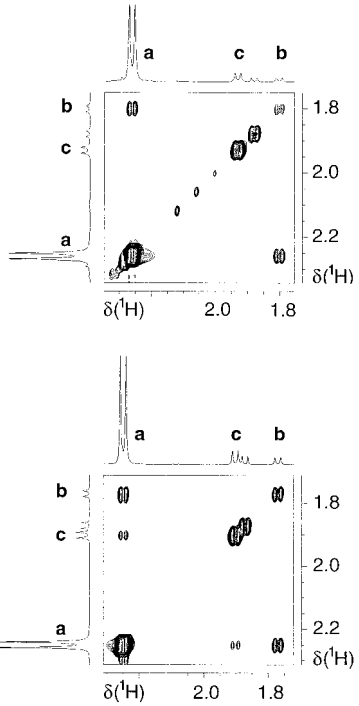

Figure 5. Sections of the NOESY spectra (500 MHz, CD_2Cl_2, room temperature, mixing time 0.8 s) of **15** (top) and **14** (bottom). Exchange between the major isomer **a** (*exo-syn-syn*) and the diastereoisomers **b** (*endo-anti-syn*) and **c** (*endo-syn-syn*) is observed only for **14**. The **a**/**c** exchange is absent in **15**.

NMR time scale. The cross-peaks in the NOESY spectra of Figure 5 clearly show that the major *exo-syn-syn* diastereoisomer **14a** is in exchange with the two minor isomers **b** and **c**. However, this is not the case for **15**, with exchange only between **15a** and the *endo-anti-syn* diastereoisomer **15b**. For this isomerization a simple $\pi-\sigma-\pi$ equilibrium may be invoked. On the other hand, full epimerization of the allyl (*exo*−*endo* equilibration) is more likely to occur via an apparent allyl rotation.[11] This requires the formation of a T-shaped intermediate (e.g., via dissociation of the pyrazolyl ligand), with subsequent rotation around the Pd−P bond and recoordination. This kind of rearrangement intuitively appears to be much more difficult for **15** than it is for **14**.

Catalytic Experiments. The new ligands **8a**,**b** and **12** have been tested in the Pd-catalyzed reaction shown in Scheme 1. The three ligands give comparably high ee's. However, some subtle differences are worth noting. The ruthenocenyl derivative **8b** gives a significantly better enantioselectivity than its ferrocenyl counterpart **8a**, when used *in situ* with the catalyst precursor [Pd_2(dba)$_3$·$CHCl_3$]. The two ligands give rise to enantiomer ratios of the product (*S*)-**1**/(*R*)-**1** of 285 and 200, respectively. The "double" ligand **12**, when added to 2 equiv of the Pd(0) precursor (one Pd center per P,N unit; i.e., a bimetallic catalyst with respect to Pd) affords the same enantioselectivity as **8b** (99.3% ee, (*S*)-**1**/(*R*)-**1** = 285), within the precision limits of the HPLC method used

(11) Gogoll, A.; Örnebro, J.; Grennberg, H.; Bäckvall, J.-E. *J. Am. Chem. Soc.* **1994**, *116*, 3631.

for selectivity determination.[1] However, the selectivity drops significantly, i.e., to an enantiomer ratio of 132 (98.5% ee), when only 0.5 equiv of Pd(0) is added to **12**. This catalyst stoichiometry is likely to generate three different species: a bimetallic and a monometallic catalyst and the free ligand. We speculate that the presence of the latter and/or an altered conformation of the monometallic catalyst is probably responsible for the lower selectivity observed. Finally, attempts to recover and reuse the bimetallic catalyst have been carried out. In order to induce the formation of Pd(II)−π-allyl species at the end of the catalytic reaction, a slight excess of **1** was used. After full consumption of benzylamine a yellow solid material could be precipitated by the addition of hexane to the concentrated reaction mixture. This material was reused without characterization or further repurification in a second catalytic run with no apparent loss of activity. However, the enantioselectivity dropped to 98.5%.

Conclusions

We have shown that ligand **12**, containing two independent P,N-chelating moieties, may be used for the preparation of a bimetallic Pd(II)−π-allyl complex in which the halves behave as essentially noncommunicating units, as indicated by the structural characterization both in the solid state and in solution. Joining covalently two equivalent mononuclear complexes that share a central ruthenocene fragment as a common substituent leads to a catalyst whose performance, in terms of activity and enantioselectivity, is indistinguishable from that of the analogous mononuclear system in the Pd-catalyzed allylic substitution of carbonate **1** with benzylamine. By virtue of its lowered solubility as compared to similar, more common mononuclear catalysts, the system containing ligand **12** bears potential as a recoverable catalyst. These combined observations suggest that the incorporation of an increasing number of "monomeric" catalyst units into structures of high molecular weight may lead to catalysts with improved properties. We are currently increasing the number of "monomeric" units incorporated into high-molecular-weight derivatives, thus extending our studies toward simple dendritic structures. Results obtained in this area will be reported in due course.

Experimental Section

General Considerations. All reactions with air- or moisture-sensitive materials were carried out under an argon or nitrogen atmosphere using standard Schlenk techniques. Freshly distilled, dry, and oxygen-free solvents were used throughout. Routine 1D ^{1}H (250.133 MHz), ^{13}C (62.90 MHz), and ^{31}P NMR (101.26 MHz) spectra were recorded using $CDCl_3$ solutions. 2D NMR experiments were carried out at either 400 or 500 MHz on 0.02 mmol samples in CD_2Cl_2. Standard pulse sequences were employed for ^{1}H 2D-NOESY,[12] ^{13}C−^{1}H,[13] and ^{31}P−^{1}H correlation studies.[14] The last two types of experiments were used for resonance assignment purposes. The phase-sensitive NOESY experiments used mixing times of 0.8 s. Elemental analyses as well as mass spectra were performed by the "Mikroelementar-analytisches Laboratorium der ETH".

Catalytic experiments (*in situ* catalysis) and determination of enantiomeric excesses were carried out as described previously.[1] A slight excess of allyl carbonate **1** (with respect to benzylamine) was used. In all experiments, conversion of the amine was quantitative, and the isolated yield of chromatographed product was ca. 90%. The procedure for catalyst recovery was as follows. When TLC indicated complete consumption of benzylamine (after ca. 12 h), THF was evaporated to half of its volume, then 2 equiv (v/v) of hexane was added. The yellow precipitate was allowed to settle, separated from the remaining solution by cannula filtration, washed with hexane (3 × 5 mL), and dried *in vacuo*. The catalyst thus recovered could be directly used for the next catalytic experiment.

(*E*)-3-(Dimethylamino)-1-ferrocenyl-2-propen-1-one (5a). Acetylferrocene (3.94 g, 17.3 mmol) was dissolved in *N*,*N*-dimethylformamide diethyl acetal (ca. 10 mL, 0.058 mol), and the mixture was heated at 125 °C until TLC showed no remaining starting material (24 h). After cooling, the solvent was evaporated *in vacuo* and the crude product crystallized from hot ethanol to yield 4.65 g (95%) of dark orange-brown **5a**, mp 170 °C. ^{1}H NMR: δ 7.67 (d, 1 H, CHN, J = 12.5 Hz), 5.33 (d, 1 H, COCH, J = 12.5), 4.75, 4.35 (s, s, 2 × 2 H, C_5H_4), 4.13 (s, 5 H, C_5H_5), 2.96 (br s, 6 H, NMe_2). ^{13}C{^{1}H} NMR: δ 191.5 (CO), 151.5 (CHN), 93.0 (CO*CH*), 82.5 (Cp C), 70.8, 68.9 (C_5H_4), 69.8 (C_5H_5), 45.0, 38.5 (NMe_2). IR (KBr): 3076 w, 2912 w, 2806 w, 1641 vs (C═O), 1552 vs (C═C), 1486 m, 1462 m, 1432 m, 1422 m, 1374 m, 1350 m, 1288 m, 1256 m, 1081 s, 1038 m, 1000 m, 976 m, 877 m, 825 m, 796 m, 767 m, 524 m, 504 m, 484 m cm^{-1}. MS (EI$^+$): m/z 283 (100, [M]$^+$), 265 (17), 240 (6, [MH − NMe_2]$^+$), 218 (5, [M − Cp]$^+$), 200 (17), 186 (19, [HFc]$^+$). Anal. Calcd for $C_{15}H_{17}FeNO$: C, 63.63; H, 6.05; N, 4.95. Found: C, 63.84; H, 6.21; N, 4.85.

(*E*)-3-(Dimethylamino)-1-ruthenocenyl-2-propen-1-one (5b). 5b was prepared analogously to **5a** from acetylruthenocene[15] (1.43 g, 5.24 mmol) in *N*,*N*-dimethylformamide diethyl acetal (ca. 10 mL, 0.058 mmol) and 44 h reaction time. The crude product was crystallized from CH_2Cl_2/hexane to yield 1.69 g (99%) of yellow **5b**, mp 167 °C. ^{1}H NMR: δ 7.63 (d, 1 H, C*H*N, J = 12.5 Hz), 5.24 (d, 1 H, COCH, J = 12.5), 5.11, 4.68 (t, t, 2 × 2 H, C_5H_4, J = 1.8), 4.53 (s, 5 H, C_5H_5), 2.96 (br s, 6 H, NMe_2). ^{13}C{^{1}H} NMR: δ 189.6 (CO), 151.3 (*C*HCO), 92.5 (CHN), 86.9 (Cp C), 72.0, 70.3 (C_5H_4), 71.5 (C_5H_5), 43.4, 38.1 (NMe_2). IR (KBr): 3080 w, 2920 w, 2806 w, 1649 vs, 1598 w, 1554 vs, 1486 m, 1463 m, 1436 m, 1373 m, 1352 m, 1291 m, 1254 m, 1212 w, 1127 w, 1100 w, 1082 s, 1027 m, 1002 m, 978 m, 925 w, 873 w, 844 w, 810 m, 800 m, 766 m, 748 w, 506 m, 470 m, 450 w, 428 m cm^{-1}. MS (EI$^+$): m/z 329 (43, [M]$^+$), 311 (33, [M − H_2O]$^+$), 296 (7, [311 − Me]$^+$), 284 (6, [M − $NHMe_2$]$^+$), 258 (13, [M − CH_2CHNMe_2]$^+$), 245 (19), 231 (31, [M − $COCHCHNMe_2$]$^+$), 205 (17), 98 (100, [$COCHCHNMe_2$]$^+$). Anal. Calcd for $C_{15}H_{17}NORu$ (328.38): C, 54.87; H, 5.22; N, 4.27. Found: C, 54.99; H, 5.12; N, 4.17.

3(5)-Ferrocenyl-1*H*-pyrazole (6a). Hydrazine hydrate (0.86 mL, 0.018 mol) was added to a solution of **5a** (2.75 g, 9.7 mmol) in EtOH (15 mL) and the mixture heated at reflux temperature for 12 h. After cooling, the solvent was removed *in vacuo*, the crude product dissolved in CH_2Cl_2, and this solution washed twice with water to remove any unreacted hydrazine and dried. Flash chromatography (hexane/ethyl acetate 2/1; R_f 0.2) yielded 2.40 g (98%) of brownish yellow **6a**, mp 146 °C. ^{1}H NMR: δ 11.1 (br s, 1 H, NH), 7.64 (br s, 1 H, Pz C^{5}H), 6.43 (br s, 1 H, Pz C^{4}H), 4.68, 4.30 (s, s, 2 × 2 H, C_5H_4), 4.07 (s, 5 H, C_5H_5). ^{13}C{^{1}H} NMR: δ 146.6 (Pz C), 134.8 (Pz C^{5}H), 102.9 (Pz C^{4}H), 76.5 (Cp C), 69.6 (C_5H_5), 68.7, 66.7 (C_5H_4). IR (KBr): 3200−2300*s* (br assoc), 1595 m, 1560 m,

(12) Jeener, J.; Meier, B. H.; Bachmann, P.; Ernst, R. R. *J. Chem. Phys.* **1979**, *71*, 4546.
(13) Summers, M. F.; Marzilli, L. G.; Bax, A. *J. Am. Chem. Soc.* **1986**, *108*, 4285.
(14) Sklenár, V.; Miyashiro, H.; Zon, G.; Miles, H. T.; Bax, A. *FEBS Lett.* **1986**, *208*, 94.
(15) Rausch, M. D.; Fischer, E. O.; Grubert, H. *J. Chem. Soc.* **1960**, *82*, 76.

1460 m, 1413 s, 1287 m, 1187 m, 1102 s, 1052 m, 1026 m, 999 m, 936 s, 871 m, 811 s, 764 s, 507 s, 483 s cm^{-1}. MS (EI^+): *m/z* 252 (100, $[M]^+$), 224 (15, $[M - N_2]^+$), 187 (8), 166 (13), 158 (53). Anal. Calcd for $C_{13}H_{12}FeN_2$ (252.10): C, 61.94; H, 4.80; N, 11.11. Found: C, 61.83; H, 4.64; N, 10.82.

3(5)-Ruthenocenyl-1*H*-pyrazole (6b). **6b** was prepared analogously to **6a** from hydrazine hydrate (0.46 mL, 9.34 mmol) and **5b** (0.7 g, 2.13 mmol) in EtOH (10 mL) and a reaction time of 24 h. Recrystallization from CH_2Cl_2/hexane yielded 508 mg (80%) of cream white **6b**, mp 185 °C. ^1H NMR: δ 12.0 (br s, 1 H, NH), 7.47 (d, 1 H, pz C^5H, $J = 2.1$ Hz), 6.24 (d, 1 H, pz C^4H, $J = 2.1$), 5.02, 4.65 (t, t, 2 × 2 H, C_5H_4, $J = 1.7$), 4.51 (s, 5 H, C_5H_5). $^{13}C\{^1H\}$ NMR: δ 134.6 (pz C^5H), 102.8 (pz C^4H), 79.8 (Cp C), 71.1 (C_5H_5), 70.4, 69.2 (C_5H_4). IR (KBr): 3250−2250 vs (br assoc), 1596 w, 1559 w, 1465 w, 1411 s, 1373 w, 1284 w, 1188 w, 1125 w, 1102 s, 1052 m, 1024 m, 996 m, 969 w, 936 m, 809 vs, 769 m, 717 w, 474 m, 424 m cm^{-1}. MS (EI^+): *m/z* 298 (100, $[M]^+$), 269 (33, $[M - N_2H]^+$), 244 (14), 231 (5, $[M - HPz]^+$), 204 (8), 167 (29, $[M - Cp - HPz]^+$). Anal. Calcd for $C_{13}H_{12}N_2Ru$ (297.32): C, 52.52; H, 4.07; N, 9.42. Found: C, 52.73; H, 4.05; N, 9.40.

1-{(*R*)-1-[(*S*)-2-(Diphenylphosphino)ferrocenyl]ethyl}-3-ferrocenyl-1*H*-pyrazole ((*R*)-(*S*)-8a). *N*,*N*-Dimethyl-(*R*)-1-[(*S*)-2-(diphenylphosphino)ferrocenyl]ethylamine ((*R*)-(*S*)-**7**[16]) (500 mg, 1.13 mmol) and **6a** (343 mg, 1.36 mmol) were dissolved in glacial acetic acid (2.5 mL) and the mixture stirred at 70 °C until TLC indicated complete conversion (8 h). The solvent was removed *in vacuo* and the orange residue chromatographed on silica (hexane/diethyl ether 3/1; R_f 0.3). Because of the marked air sensitivity of (*R*)-(*S*)-**8a** (oxidation at phosphorus), chromatography had to be carried out under argon. Yield: 545 mg (74%) as dark orange crystals (from hexane). Mp: 112−113 °C. $[\alpha]_D^{23} = -246$ ($CHCl_3$, $c = 0.39$). ^1H NMR: δ 7.57 (m, 2 Ph H), 7.39 (m 3 Ph H), 7.03 (m 3 Ph H), 6.87 (d, 1 H, Pz C^5H, $J = 2.3$ Hz), 6.86 (m 2 Ph H), 5.79 (dq, 1 H, C*H*MeN, $J = 6.9, 3.2$), 5.72 (d, 1 H, Pz C^4H, $J = 2.3$), 4.72, 4.54, 4.48, 4.42 (m 4 × 1 Cp H), 4.16 (m 2 Cp H), 4.04 (s, 5 H, C_5H_5), 3.96 (m 1 Cp H), 3.93 (s, 5 H, C_5H_5 (Pz)), 1.93 (d, 3 H, CH*Me*N, $J = 6.9$). $^{13}C\{^1H\}$ NMR: δ 149.2 (Pz C), 139.2, 137.8 (Ph C), 135.4−127.4 (Ph CH), 129.1 (Pz C^5H), 102.2 (Pz C^4H), 93.6 (d, Cp C, $J = 26$ Hz), 79.6 (Cp C), 76.2 (d, Cp C, $J = 11.9$), 72.1, 69.8, 67.9, 66.6 (Cp CH), 69.9, 69.3 (C_5H_5), 55.8 (d, *C*HMeN, $J = 9.9$), 21.7 (CH*Me*N). $^{31}P\{^1H\}$ NMR: δ −25.5 (*s*). IR (KBr): 3046 w, 2978 m, 1554 m, 1478 m, 1433 s, 1405 m, 1369 m, 1314 m, 1246 m, 1217 m, 1168 m, 1105 s, 1048 m, 1026 m, 1000 s, 870 m, 820 s, 744 s, 696 s, 504 s, 483 s cm^{-1}. MS (EI^+): *m/z* 648 (92, $[M]^+$), 583 (9, $[M - Cp]^+$), 517 (7, $[M - HCp_2]^+$), 397 (45, $[M - HPz]^+$), 372 (29), 324 (18), 252 (96, $[HPz]^+$), 212 (100, $[M - HPz - PPh_2]^+$). Anal. Calcd for $C_{37}H_{33}Fe_2N_2P$ (648.35): C, 68.54; H, 5.13; N, 4.32. Found: C, 68.63; H, 5.33; N, 4.25.

1-{(*R*)-1-[(*S*)-2-(Diphenylphosphino)ferrocenyl]ethyl}-3-ruthenocenyl-1*H*-pyrazole ((*R*)-(*S*)-8b). **8b** was prepared analogously to **8a** from (*R*)-(*S*)-**7** (286 mg, 0.65 mmol) and **6b** (251 mg, 0.84 mmol) in glacial acetic acid (2 mL), at 70 °C for 20 h. The orange residue was chromatographed under Ar on silica (hexane/diethyl ether 4/1; R_f 0.1). Yield: 259 mg (61%) as an orange solid. Mp: 164 °C. $[\alpha]_D^{23} = -211$ ($CHCl_3$, $c = 0.31$). $^{31}P\{^1H\}$ NMR: δ −25.6. ^1H NMR: δ 7.55 (m, 2 Ph H), 7.37 (m, 3 Ph H), 7.09−6.98 (m, 3 Ph H), 6.83−6.76 (m, 3 H, pz C^5H, 2 Ph H), 5.71 (dq, 1 H, C*H*MeN, $J = 6.9, 3.2$ Hz), 5.56 (d, 1 H, pz C^4H, $J = 2.3$), 4.88, 4.53 (2 × m, 2 × 2 H, C_5H_4), 4.69, 4.39, 3.91 (q, t, t, 3 × 1 H, C_5H_3), 4.36 (s, 5 H, Rc C_5H_5), 4.01 (s, 5 H, Fc C_5H_5), 1.89 (d, 3 H, CH*Me*N, $J = 6.9$). $^{13}C\{^1H\}$ NMR: δ 148.1, 139.0−127.0 (Ar C, CH), 102.5 (pz C^4H), 93.4, 83.4, 76.9 (Cp C), 71.7, 71.6 (C_5H_3), 70.8 (Rc C_5H_5), 69.6, 69.4 (C_5H_4), 69.6 (Fc C_5H_5), 55.5 (*C*HMeN), 21.3 (CH*Me*N). IR (KBr): 3080 w, 2985 w, 2941 w, 1654 w, 1585 w, 1560 w, 1482 m, 1434 m, 1402 m, 1368 m, 1317 w, 1244 m, 1215 m, 1167 m, 1101 m, 1050 m, 1026 w, 1001 m, 975 m, 871 w, 826 s, 801 s, 745 vs, 698 vs, 502 m, 472 s, 454 m, 426 m cm^{-1}. MS (EI^+): *m/z* 694 (14, $[M]^+$), 629 (6, $[M - Cp]^+$), 418 (4), 396 (17, $[M - HPzRu(Cp)_2]^+$), 353 (21), 331 (23, $[M - Cp - HPzRu(Cp)_2]^+$), 298 (15, $[HPzRu(Cp)_2]^+$), 275 (25, $[M - FeCp - HPzRu(Cp)_2]^+$), 212 (37, $[M - PPh_2 - PzRu(Cp)_2]^+$), 183 (69, $[M - PPh_2 - EtPzRu(Cp)_2]^+$), 121 (100, $[FeCp]^+$). Anal. Calcd for $C_{37}H_{33}FeN_2PRu$ (693.57): C, 64.08; H, 4.80; N, 4.04. Found: C, 64.33; H, 4.96; N, 4.00.

1,1′-Bis[(*E*)-3-(dimethylamino)-2-propenoyl]ruthenocene (10). 1,1′-Diacetylruthenocene[15] (2.50 g, 7.9 mmol) was dissolved in *N*,*N*-dimethylformamide diethyl acetal (*ca.* 10 mL, 0.058 mol), and the mixture was heated at 125 °C until TLC showed no starting material (40 h). After cooling, the solvent was evaporated *in vacuo* and the crude product chromatographed on silica (CH_2Cl_2/MeOH 8/1; R_f 0.3) to yield 2.05 g (62%) of bright yellow **10**, mp 232 °C. ^1H NMR: δ 7.57 (d, 2 H, CHN, $J = 12.5$), 5.14 (d, 2 H, COCH, $J = 12.5$ Hz), 5.06, 4.66 (t, t, 2 × 4 H, C_5H_4), 2.95 (br s, 12 H, NMe_2). $^{13}C\{^1H\}$ NMR: δ 188.9 (CO), 151.7 (CHN), 93.1 (CO*CH*), 88.5 (Cp C), 74.0, 72.1 (C_5H_4), 44.7, 37.2 (NMe_2). IR (KBr): 3082 w, 2901 w, 2803 w, 1641 vs (C═O), 1553 vs (C═C), 1487 m, 1458 m, 1434 s, 1375 m, 1346 m, 1288 m, 1253 s, 1081 s, 1029 m, 803 m, 762 m, 507 m, 499 m, 477 m cm^{-1}. MS (EI^+): *m/z* 426 (24, $[M]^+$), 408 (11), 390 (4), 354 (5), 340 (6), 327 (12), 311 (6), 298 (12), 284 (7), 270 (9), 256 (7), 245 (8), 231 (8), 167 (10), 98 (100, $[COCHCHNMe_2]^+$). Anal. Calcd for $C_{20}H_{24}N_2O_2Ru$ (425.49): C, 56.46; H, 5.69; N, 6.58. Found: C, 56.50; H, 5.96; N, 6.29.

1,1′-Bis(3(5)-1*H*-pyrazolyl)ruthenocene (11). Hydrazine hydrate (0.34 mL, 7.05 mmol) was added to a suspension of **10** (1.50 g, 3.53 mmol) in EtOH (8 mL) and the mixture heated at reflux temperature until the yellow color of **10** had completely disappeared. After cooling, the poorly soluble product was filtered off and thoroughly washed with water, EtOH, and CH_2Cl_2. Yield: 1.11 g (85%) of **11**·$0.5H_2O$ as a cream white solid. Mp: 233−234 °C. ^1H NMR: δ 7.48 (d, 2 H, pz C^5H, $J = 1.9$ Hz), 6.19 (d, 2 H, pz C^4H, $J = 1.9$), 5.26 (br s, 2 NH), 5.03, 4.92, 4.64, 4.60 (4 × t, 4 × 2 H, C_5H_4, $J = 1.7$), 1.60 (br s, 1 H, H_2O). $^{13}C\{^1H\}$ NMR: δ 102.9 (pz C^4H), 71.9, 71.2, 70.2, 69.8 (C_5H_4); no other signals detectable due to low solubility. IR (KBr): 3250−2200 vs (br assoc), 1647 w, 1598 m, 1557 m, 1461 m, 1412 s, 1367 m, 1285 m, 1183 m, 1125 m, 1098 m, 1056 m, 1021 m, 965 m, 932 s, 808 s, 771 s, 485 m cm^{-1}. MS (EI^+): *m/z* 364 (100, $[M]^+$), 354 (76, $[M(H_2O) - N_2]^+$), 335 (19), 325 (20), 309 (12), 297 (34), 269 (14), 256 (6). Anal. Calcd for $C_{16}H_{14}N_4Ru$·$0.5H_2O$ (372.39): C, 51.61; H, 4.06; N, 15.05. Found: C, 51.67; H, 4.01; N, 15.47.

1,1′-Bis[1-(1-{(*R*)-1-[(*S*)-2-(diphenylphosphino)ferrocenyl]ethyl})-1*H*-pyrazol-3-yl]ruthenocene ((*R*,*R*)-(*S*,*S*)-12). (*R*)-(*S*)-**7** (668 mg, 1.51 mmol) and **11** (250 mg, 0.69 mmol) were suspended in glacial acetic acid (1.5 mL), and the mixture was stirred at 75−80 °C until TLC indicated complete conversion (12 h). The solvent was removed *in vacuo* and the orange residue chromatographed on silica (hexane/EtOAc 3/1; R_f 0.2). Yield: 280 mg (35%) of (*R*,*R*)-(*S*,*S*)-**12** as a yellow solid. Mp: 88−89 °C. $[\alpha]_D^{23} = -222$ ($CHCl_3$, $c = 0.21$). $^{31}P\{^1H\}$ NMR (202 MHz, CD_2Cl_2): δ −23.7. ^1H NMR (500 MHz, CD_2Cl_2): δ 7.57 (m, 4 Ph H), 7.39 (m, 6 Ph H), 7.09−6.95 (m, 6 Ph H), 6.83 (d, 2 H, pz C^5H, $J = 2.3$ Hz), 6.73 (m, 4 Ph H), 5.64 (dq, 2 H, C*H*MeN, $J = 6.9, 3.1$), 5.41 (d, 2 H, pz C^4H, $J = 2.3$), 4.72 (m, 2 Fc H), 4.65, 4.58 (m, 2 × 2 Rc H), 4.41 (t, 2 Fc H), 4.35 (m, 4 Rc H), 4.02 (s, 10 H, C_5H_5), 3.91 (m, 2 Fc H), 1.87 (d, 6 H, CH*Me*N, $J = 6.9$). $^{13}C\{^1H\}$ NMR (63 MHz, $CDCl_3$): δ 148.3 (pz C), 139.1−127.3 (Ph C, CH), 129.1 (pz C^5H), 102.9 (pz C^4H), 93.9 (Cp C), 84.0, 76.1 (Cp C), 71.9, 71.1, 70.8, 69.6 (Cp CH), 69.9 (C_5H_5), 55.6 (*C*HMeN), 21.6 (CH*Me*N). IR (KBr): 3049 w, 2925 m, 1734 w, 1654 w, 1558 m, 1493 m, 1478 m, 1433 s, 1401 m, 1369 m, 1310 m, 1245 m, 1167 m, 1106 m, 1048 m, 1026 m, 1001 m, 819 s, 743 vs, 697 vs, 503 m, 483 s, 456 m cm^{-1}. MS (EI^+): *m/z* 1156 (42, $[M]^+$), 1079 (2, $[M - Ph]^+$),

(16) Hayashi, T.; Mise, T.; Fukushima, M.; Kagotani, M.; Nagashima, N.; Hamada, Y.; Matsumoto, A.; Kawakami, S.; Konishi, M.; Yamamoto, K.; Kumada, M. *Bull. Chem. Soc. Jpn.* **1980**, *53*, 1138.

815 (15), 759 (11, [M − PPF]$^+$) 693 (4, [M − PPFPz]$^+$), 539 (70), 397 (100, [PPF]$^+$), 331 (56, [397 − HCp]$^+$), 276 (84, [331 − Fe]$^+$), 212 (96, [FcCH=CH_2]$^+$). Anal. Calcd for $C_{64}H_{56}Fe_2N_4P_2Ru$ (1155.88): C, 66.50; H, 4.88; N, 4.85. Found: C, 66.21; H, 5.16; N, 4.64.

[Pd(η^3-PhCHCHCHPh)((*R*)-(*S*)-8a)][PF_6] (13). To a solution of (*R*)-(*S*)-**8a** (180 mg, 0.278 mmol) in acetone (20 mL) was added [Pd(η^3-PhCHCHCHPh)(μ-Cl)]$_2$[9] (77.5 mg, 0.116 mmol). The mixture was stirred for 15 min, after which time solid $TlPF_6$ (80.8 mg, 0.231 mmol) was added and stirring continued for 1 h. The suspension was filtered through a pad of Celite, the solvent evaporated *in vacuo* except for a few milliliters, and the product precipitated with hexane. Repeated filtration and precipitation yielded 248 mg (98%) of (*R*)-(*S*)-**13** as an orange microcrystalline solid. IR (KBr): 3055 w, 1555 m, 1491 m, 1435 m, 1311 m, 1243 m, 1161 m, 1107 m, 1074 m, 1053 m, 1001 m, 840 vs (PF_6), 754 s, 696 s, 557 s, 529 m, 503 m, 467 m cm^{-1}. MS (FAB$^+$) *m*/*z* 1092 (2.2, [MPF_6]$^+$), 947 (100, [M]$^+$), 826 (11, [M − FeCp]$^+$), 754 (39, [M − PhCHCHCHPh]$^+$). Anal. Calcd for $C_{52}H_{46}F_6Fe_2N_2P_2Pd$ (1093.00): C, 57.14; H, 4.24; N, 2.56. Found: C, 57.05; H, 4.51; N, 2.51.

[Pd(η^3-PhCHCHCHPh)((*R*)-(*S*)-8b)][PF_6] ((*R*)-(*S*)-14). **14** was prepared analogously to **13** from (*R*)-(*S*)-**8b** (250 mg, 0.36 mmol), [Pd(η^3-PhCHCHCHPh)(μ-Cl)]$_2$ (60.4 mg, 0.090 mmol), and $TlPF_6$ (63.0 mg, 0.18 mmol) in acetone (20 mL). Yield: 195 mg (95%) of (*R*)-(*S*)-**14** as a dark orange microcrystalline solid. IR (KBr): 3055 w, 2925 w, 1631 w, 1553 m, 1492 m, 1436 m, 1404 m, 1311 m, 1243 m, 1214 w, 1162 m, 1102 m, 1073 m, 1053 m, 999 m, 840 vs (PF_6), 753 s, 696 s, 558 s, 502 s, 468 s cm^{-1}. MS (FAB$^+$): *m*/*z* 1138 (2, [MPF_6]$^+$), 993 (100, [M]$^+$), 799 (27, [M − $PhCH_2CHCHPh$]$^+$). Anal. Calcd for $C_{52}H_{46}F_6FeN_2P_2PdRu$ (1138.22): C, 54.87; H, 4.07; N, 2.46. Found: C, 54.86; H, 4.22; N, 2.45. For NMR characterization, see Table 3 and the Supporting Information.

[{Pd(η^3-PhCHCHCHPh)}$_2${(*R*,*R*)-(*S*,*S*)-12}][PF_6]$_2$ ((*R*,*R*)-(*S*,*S*)-15). **15** was prepared analogously to **13** from (*R*,*R*)-(*S*,*S*)-**12** (100 mg, 0.087 mmol), [Pd(η^3-PhCHCHCHPh)(μ-Cl)]$_2$ (58.0 mg, 0.087 mmol), and $TlPF_6$ (60.4 mg, 0.173 mmol) in acetone (10 mL). Yield: 176 mg (99%) of (*R*,*R*)-(*S*,*S*)-**15** as a yellow microcrystalline solid. IR (KBr): 3055 w, 2951 w, 2929 w, 1554 m, 1491 m, 1436 m, 1404 m, 1374 w, 1310 m, 1243 m, 1215 m, 1161 m, 1099 m, 1074 m, 1053 m, 1001 m, 840 vs (PF_6), 754 s, 695 s, 557 s, 525 m, 502 s, 466 m cm^{-1}. MS (FAB$^+$): *m*/*z* 1900 (74, [MPF_6]$^+$), 1561 (41, [M − PhCHCHCHPh]$^+$), 1455 (32, [1561 − Pd]$^+$), 1369 (24), 1264 (11, [1455 − PhCHCHCHPh]$^+$), 878 (100, [PPFPz(CpRu)$PdPF_6$]$^+$), 780 (16). Anal. Calcd for $C_{94}H_{82}F_{12}Fe_2N_4P_4Pd_2Ru$ (2045.19): C, 55.20; H, 4.04; N, 2.74. Found: C, 55.08; H, 4.35; N, 2.66. For NMR characterization, see Table 3 and the Supporting Information.

X-ray Structure Analysis of (*R*)-(*S*)-14 and (*R*,*R*)-(*S*,*S*)-15. Orange single crystals of (*R*)-(*S*)-**14** were obtained from MeOH at −20 °C. An octahedron-shaped one was mounted in a glass capillary. Orange needles of (*R*,*R*)-(*S*,*S*)-**15** suitable for X-ray analysis were obtained from CH_2Cl_2/EtOH at room temperature. Because of fast decay when taken out of the mother liquor (loss of enclosed CH_2Cl_2), the selected crystal had to be sealed in a glass capillary containing a saturated CH_2Cl_2/EtOH solution of (*R*,*R*)-(*S*,*S*)-**15**. For both compounds, data were measured with variable scan speed to ensure constant statistical precision on the collected intensities. One standard reflection was measured every 120 reflections; no significant variation was detected. For **15**, measurement had to be stopped at $2\theta = 35°$, because of crystal decay (loss of solvent). Selected crystallographic and relevant data collection parameters are listed in Table 1. The structures were solved with Patterson methods and refined by full-matrix least squares using anisotropic displacement parameters for all non-hydrogen atoms, in the case of **14**, and for all Pd, Ru, Fe, P, and F atoms for **15**. For this compound all carbon rings as well as the PF_6 counteranions were refined as rigid groups. Solvent molecules found in the crystal packing were highly disordered and were therefore refined without constraints. Hydrogen atoms were refined in idealized positions (riding model with fixed isotropic $U = 0.080$ Å^2). Maximum and minimum difference peaks were 0.81 and −0.35 e Å^{-3} (**14**) and 0.49 and −0.47 e Å^{-3} (**15**). All calculations were carried out by using the Siemens SHELXTL PLUS system.

Acknowledgment. U.B. is grateful to Lonza Ltd. for financial support. We thank Paul S. Pregosin for most valuable discussions concerning 2D NMR spectroscopy.

Supporting Information Available: Tables of crystallographic parameters, atomic coordinates, all bond distances and angles, anisotropic displacement coefficients, and coordinates of hydrogen atoms for **14** and **15**, text and figures giving a complete NMR data set for **14** and **15**, including a section of the 500 MHz ^{1}H spectrum showing the presence of different isomers and a section of the 500 MHz ^{1}H NOESY spectra of the two compounds essential for conformation assignment of **15**, and a table giving cyclic voltammetry data for compounds **8b**, **12**, **14**, and **15** (30 pages). Ordering information is given on any current masthead page. Tables of calculated and observed structure factors (21 pages) for both compounds may be obtained from the authors upon request.

OM970532X